LETTERS

The structural basis for activation of plant immunity by bacterial effector protein AvrPto

Weiman Xing[1,2], Yan Zou[1,3]*, Qun Liu[4]*, Jianing Liu[1], Xi Luo[1], Qingqiu Huang[3], She Chen[1], Lihuang Zhu[3], Ruchang Bi[2], Quan Hao[4], Jia-Wei Wu[5], Jian-Min Zhou[1] & Jijie Chai[1]

Pathogenic microbes use effectors to enhance susceptibility in host plants. However, plants have evolved a sophisticated immune system to detect these effectors using cognate disease resistance proteins[1], a recognition that is highly specific, often elicits rapid and localized cell death, known as a hypersensitive response, and thus potentially limits pathogen growth[2–5]. Despite numerous genetic and biochemical studies on the interactions between pathogen effector proteins and plant resistance proteins, the structural bases for such interactions remain elusive. The direct interaction between the tomato protein kinase Pto and the *Pseudomonas syringae* effector protein AvrPto is known to trigger disease resistance and programmed cell death[6,7] through the nucleotide-binding site/leucine-rich repeat (NBS-LRR) class of disease resistance protein Prf[8]. Here we present the crystal structure of an AvrPto–Pto complex. Contrary to the widely held hypothesis that AvrPto activates Pto kinase activity, our structural and biochemical analyses demonstrated that AvrPto is an inhibitor of Pto kinase *in vitro*. The AvrPto–Pto interaction is mediated by the phosphorylation-stabilized P+1 loop and a second loop in Pto, both of which negatively regulate the Prf-mediated defences in the absence of AvrPto in tomato plants. Together, our results show that AvrPto derepresses host defences by interacting with the two defence-inhibition loops of Pto.

The *Pseudomonas syringae* pv. *tomato* effector proteins AvrPto and AvrPtoB—on injection into host cells by the type III secretion system[9–11]—promote virulence in susceptible plants, but triggers disease resistance in tomato plants carrying Pto[6,7,12], a serine/threonine protein kinase, and Prf[8], a Pto-interacting[13] protein. It is widely thought that interaction of AvrPto with Pto stimulates Pto kinase activity and thereby initiates resistance[5,13–15]. However, direct evidence for this hypothesis is lacking *in vivo* or *in vitro*. In contrast, one recent finding indicated that AvrPto may act as a suppressor of Pto-like kinases or Pto-like receptor kinases for suppressing MAP kinase (MAPK)-mediated basal defences[16]. An important finding contributing to understanding Pto signalling showed that Pto negatively regulates Prf-mediated resistance[15]. How AvrPto relieves this inhibition and triggers disease resistance remains elusive.

To elucidate the mechanism by which AvrPto initiates disease resistance, we determined the crystal structure of the AvrPto–Pto complex (Supplementary Fig. 1 and Supplementary Table 1). AvrPto binds Pto at a 1:1 ratio (Fig. 1a) with a binding affinity of about 0.11 μM (Supplementary Fig. 2). The interaction is primarily mediated by the contacts of one end of an AvrPto helical bundle with one Pto loop preceding β1 (Fig. 1a, b, the first interface) and the AvrPto GINP (Gly-Ile-Asn-Pro) motif with the Pto P+1 loop (Fig. 1a, c, the second interface). Compared to its solution structure[17], AvrPto in the complex remains essentially unchanged except that the GINP motif becomes well-ordered on binding to Pto (Supplementary Fig. 3). Dali search identified three kinases, cAMP-dependent protein kinase A (PKA), TGF-β receptor I (TβRI) and check point kinase 1 (CHK1) as the closest structural homologues to Pto.

Hydrophobic contacts primarily mediate the interaction around the first interface. Pto(V51) makes hydrophobic contacts with residues AvrPto(Y89, M90, L101, P102) (Fig. 1b), the importance of which was confirmed by the binding assay (Supplementary Fig. 4). In addition to Pto(H49, V51), Pto(F52) makes van der Waals contacts with AvrPto and their importance in AvrPto–Pto interaction was corroborated by mutational analysis (Fig. 1d). Fen, a closely

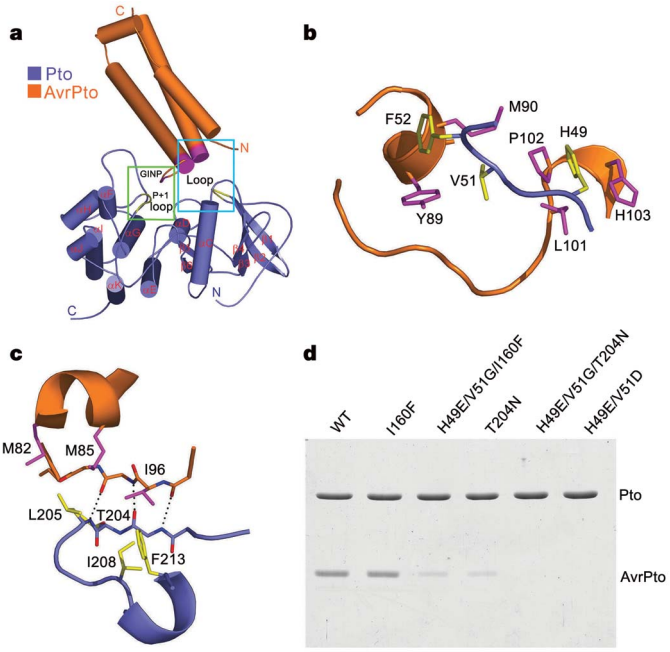

Figure 1 | Bipartite AvrPto–Pto interfaces. a, Overall structure of the AvrPto–Pto complex. Yellow, the Pto P+1 loop and the loop preceding β-1; magenta, the AvrPto GINP motif and its end of helical bundle. The first and second interfaces are highlighted in cyan and green frames, respectively. **b**, Detailed interactions between the loop preceding β-1 in Pto and the end of helical bundle of AvrPto (the first interface). **c**, Detailed interactions between the Pto P+1 loop and the AvrPto GINP motif (the second interface). **d**, Effects of point mutations in Pto on the interaction with AvrPto. WT, wild type.

[1]National Institute of Biological Sciences, No. 7 Science Park Road, Beijing 102206, China. [2]Institute of Biophysics, [3]Institute of Genetics and Developmental Biology, Chinese Academy of Sciences, Beijing 100101, China. [4]Cornell High-Energy Synchrotron Source, Cornell University, Ithaca, New York 14853, USA. [5]Department of Biological Sciences and Biotechnology, Tsinghua University, 100084, Beijing, China.
*These authors contributed equally to this work.

related Pto family member, contains Glu and Gly at H49 and V51 (Supplementary Fig. 5), respectively, and does not interact with AvrPto[18]. Incorporation of these two substitutions in Pto always resulted in a spontaneous mutation elsewhere in the protein probably owing to its toxicity to *Escherichia coli*. Nonetheless, one of these resultant mutants, Pto(H49E/V51G/I160F), was significantly compromised in its interaction with AvrPto (Fig. 1d).

Both hydrogen bonds and hydrophobic interaction contribute to the second interface. Three residues of the AvrPto GINP motif interact with the Pto P+1 loop through three main chain hydrogen bonds (Fig. 1c), whereas AvrPto(I96) packs against the hydrophobic residues Pto(I208, L205, F213) (Fig. 1c). The role of the second interface in the hypersensitive response was further confirmed by *Agrobacterium*-mediated transient assay (Supplementary Fig. 6a). Pto(T204), proposed to be the structural determinant of Pto for specific recognition of AvrPto[19], exhibited a weak interaction with AvrPto when mutated to Asn (Fig. 2d). However, substitution of all three residues in Pto—Pto(H49E/V51G/T204N)—completely abolished its interaction with AvrPto (Fig. 1d), indicating that the recognition specificity of AvrPto by Pto is conferred by these three residues. In agreement with this, AvrPto had no effect on the ability of Pto(H49E/V51G/T204N) to trigger the hypersensitive response (Supplementary Fig. 6b). Although H49 is substituted with Ala in *Lycopersicon hirsutum* Pto (Supplementary Fig. 4), it still binds AvrPto[20], because the second interface still remains intact.

The P+1 loop of Pto adopts a conformation similar to those of active PKA and CHK1 but different from that of the inactive form of TβRI (Fig. 2a), indicating that Pto in the complex assumes an active conformation. Its activation segment is stabilized through hydrogen bonds and hydrophobic interactions (Fig. 2b). Like many RD kinases[21,22], which contain an arginine (R) preceding the catalytic aspartate (D) in the catalytic loop, phosphorylation of the Pto activation loop is critical in determining its active form. Both electron density around Pto(T199) (Fig. 2c) and mass spectrometry data (not shown) indicated that this residue had been phosphorylated in the crystal. As with other RD kinases (Supplementary Fig. 7), phosphorylation of Pto(T199) to p-Pto(T199) has an important role in maintaining Pto in the active conformation by forming salt bridges with Pto(R163) and Pto(K187) (Fig. 2c). Supporting a role of p-Pto(T199) in Pto kinase activity, mutation of this residue significantly compromised Pto autophosphorylation (Fig. 2d) and phosphorylation of the substrate Pti1 (Supplementary Fig. 8b). A higher level of kinase activity of the same mutant in a previous study[23] probably resulted from usage of a preferred Pto cofactor, $MnCl_2$ (Supplementary Fig. 8a). Pto(Y207) is also important for stabilizing the P+1 loop by making hydrophobic contacts with Pto(V229, I241) and the aliphatic portion of Pto(K166), and hydrogen bonding with Pto(E233, S167) (Fig. 2b).

To investigate if the active conformation of Pto is required for AvrPto–Pto interaction, we mutated residues that stabilize the P+1 loop (Fig. 2b) and examined their kinase activity and interaction with AvrPto. One of these residues, Pto(S226), immediately underneath the P+1 loop, supports the loop in the proper conformation (Fig. 2b). Pto(S226D) had completely abolished kinase activity and interaction with AvrPto (Fig. 2d). An interaction between Pto(T199A) and AvrPto was not detected by Coomassie blue staining (Fig. 2d) but by the more sensitive silver staining, indicating a weak interaction (Supplementary Fig. 9), consistent with previous study[23]. These results suggest that the phosphorylation-stabilized P+1 is important for AvrPto–Pto interaction. Consistently, Pto(R163A) disrupting a salt bridge (Fig. 2c) abolished its interaction with AvrPto in this (Fig. 2d)

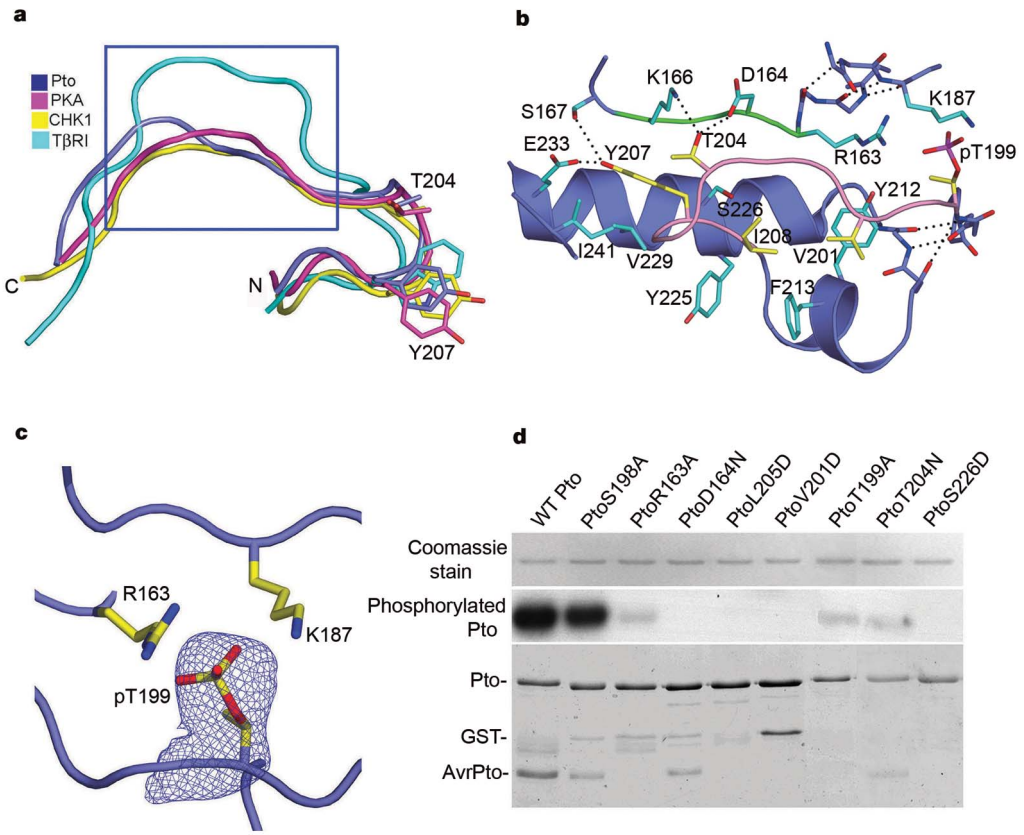

Figure 2 | The active conformation of Pto is important for AvrPto binding. **a**, Structural alignment of the Pto P+1 loop (highlighted in the blue frame) with those of kinases PKA, CHK1 and TβR1. **b**, Hydrogen bonds and hydrophobic contacts are involved in maintaining the Pto activation segment in the active conformation. The catalytic loop and activation segment of Pto are coloured in green and pink, respectively. **c**, Omit electron density map for the phosphorylated Pto(T199) (shown at 1.2 σ). **d**, Effects of various Pto mutations on kinase activity and interaction with AvrPto. The mutant Pto(L205D) (ref. 15) is a negative control. GST, glutathione *S*-transferase.

and a previous study[15]. A role of p-Pto(T199) in AvrPto-triggered hypersensitive response was supported by the observation[23] that Pto(T199A) decreased AvrPto-triggered hypersensitive response. The importance of p-Pto(T199) for AvrPto recognition is consistent with previous findings that Pto mutants abolishing the kinase activity also eliminated their interaction with AvrPto[6,7,14,15,23]. However, an exception to this has been reported. The kinase-deficient mutant Pto(D164N) still interacts with AvrPto, as shown in a previous[14] and this (Fig. 2d) study. This may have resulted from the introduction of one hydrogen bond between oxygen OD1 of Asn and the amide nitrogen of Pto(T204), thus stabilizing the Pto P+1 loop and enabling the interaction with AvrPto. Consistent with this possibility, Pto(D164A) exhibited no interaction with AvrPto[15]. To support further the important role of p-Pto(T199) in Pto recognition of AvrPto, *trans*-phosphorylation of Pto(T199) in the kinase-deficient mutant Pto(K69H) by the wild-type Pto (Supplementary Fig. 10) restored the ability of this mutant to interact with AvrPto (Supplementary Fig. 11). These results indicate that p-Pto(T199) rather than the kinase activity itself is important for Pto recognition of AvrPto.

Previous studies identified a number of constitutive gain-of-function (CGF) Pto mutants that elicit AvrPto-independent but Prf-dependent hypersensitive response[14,15]. Our structure indicates that many of these mutations destabilize the P+1 loop of Pto. In addition, all of the CGF mutants in the P+1 loop abolished or greatly reduced Pto kinase activity (Supplementary Fig. 12). These results suggest that proper conformation around the Pto P+1 loop region is important for inhibition of Prf-dependent hypersensitive response. To verify this, we tested CGF hypersensitive response activity of two Pto derivatives—Pto(S226D) and Pto(V201D)—carrying substitutions in residues that stabilize the P+1 loop from outside (Fig. 2b). These two mutants exhibited no kinase activity *in vitro* and had impaired interactions with AvrPto (Fig. 2d). As expected, both mutants exhibited strong CGF hypersensitive response activity (Fig. 3a). Contrary to Pto(Y207D) (ref. 14), the mutant Pto(Y207F), like Pto(Y207W) (ref. 14), did not exhibit CGF hypersensitive response activity (Fig. 3c), because Phe can still form hydrophobic contacts with Pto(V229, I241) and the aliphatic portion of Pto(K166) (Fig. 2b), thus stabilizing the P+1 loop.

To examine the *in vivo* importance of the first interface in elicitation of a hypersensitive response, we generated mutants Pto(H49E/V51G, H49D/V51D) and transiently expressed them in *Nicotiana benthamiana*. Strikingly, these two mutants also elicited a CGF hypersensitive response (Fig. 3b), indicating that, like the P+1 loop, this loop also exerts an inhibitory effect on the hypersensitive response. In full support of the *in vivo* importance of this interface, overexpression of Fen in *N. benthamiana* phenocopies the hypersensitive response induced by these two mutants[18]. As with CGF mutants in the P+1 loop, these two mutants were also significantly compromised in their interaction with AvrPto (Fig. 1d).

Structural comparison reveals that the interaction of Pto with the AvrPto GINP motif is similar to that of PKA with its pseudosubstrate PKI (Fig. 4a), a peptide inhibitor of PKA[24], arguing against the possibility that AvrPto promotes Pto kinase activity. To test this, we examined the kinase activity of Pto in the presence of AvrPto. Pto autophosphorylation (Fig. 4b) and phosphorylation towards a substrate Pti1 (Fig. 4c) were significantly reduced in the presence of AvrPto, with a half-maximal inhibition of Pti1 phosphorylation at about 11 μM (Supplementary Fig. 13). The inhibitory effect apparently resulted from AvrPto–Pto interaction, because AvrPto(Y89D) (Fig. 4d) and Pto(H49D/V51D) (Fig. 4e), which do not interact with their wild-type partners, showed little impact on Pto kinase activity, indicating that binding of AvrPto consequently inhibits the Pto kinase activity.

Defences are unlikely to be initiated by AvrPto inhibition of Pto kinase, because Pto(H49D/V51D), which is insensitive to kinase inhibition by AvrPto (Fig. 4e), constitutively activates the hypersensitive response in plants (Fig. 3b). It is logical to conclude that it is the AvrPto–Pto interaction, rather than the altered kinase activity, that activates Prf. Mutations that disrupt proper conformation around the P+1 loop region can relieve its inhibition and generate a CGF hypersensitive response without the requirement for Pto kinase activity (Fig. 3a and ref. 15). However, Pto kinase activity is required for AvrPto-triggered resistance[6,7,14,15,23]. In addition to recognizing AvrPto (Fig. 2d), Pto kinase activity seems to be critical downstream of recognition for induction of disease resistance, because the autophosphorylation site Pto(S198) was shown to be required for elicitation of a hypersensitive response (ref. 23) but dispensable for interaction with AvrPto (Fig. 2d and ref. 23). It is possible that p-Pto(S198) is involved in Pto conformational changes critical for Pto signalling[13] (Supplementary Fig. 14). A very recent study showed that Prf and Pto form a complex *in vivo* in which Pto probably acts as a switch for hypersensitive response induction[13]. The two AvrPto-interacting loops in Pto negatively regulate the hypersensitive response (Fig. 3), probably by direct or indirect interaction with Prf. On the other hand, Pto apparently plays a positive part in activating Prf, because plants lacking Pto do not trigger disease resistance[5]. We propose that the two loops of Pto act as a lock to keep Prf in the inactive state, whereas binding of AvrPto unlocks them and allows conformational changes in Pto, altering the way Pto interacts with Prf and consequently activating Prf (Supplementary Fig. 14).

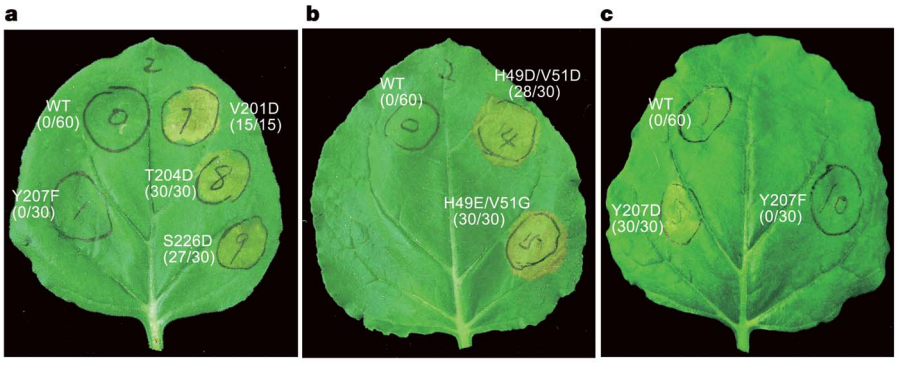

Figure 3 | Mutations in the two AvrPto–Pto interfaces trigger a CGF hypersensitive response in *N. benthamiana*. **a**, Transient expression of Pto mutants—Pto(Y207F, V201D, T204D, S226D)—with mutations in the residues that are important for maintaining the conformation of P+1 in *Nicotiana benthamiana*. The mutant Pto(T204D) is a positive control (ref. 15). **b**, Transient expression of Pto mutants Pto(H49D/V51D) and Pto(H49E/V51G) with mutations in the residues that are important for the AvrPto–Pto interaction in the first interface (Fig. 1b). **c**, Transient expression of Pto(Y207) mutants Pto(Y207F, Y207D) that stabilize the P+1 loop through hydrophobic contacts (Fig. 2b). The numbers in brackets indicate the number of leaves showing the symptoms of a hypersensitive response divided by the total number of leaves infiltrated with the indicated plasmid.

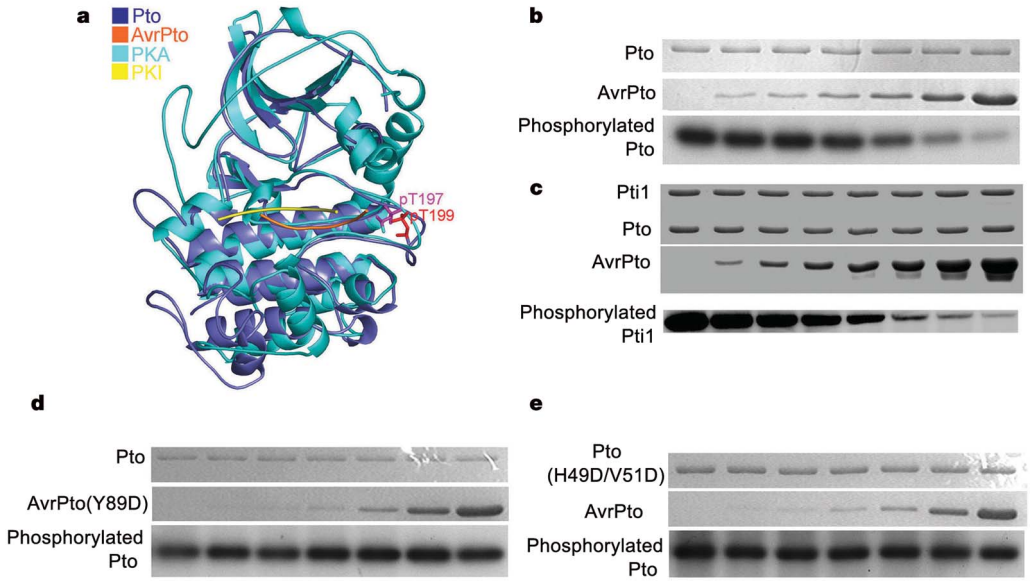

Figure 4 | AvrPto inhibits the kinase activity of Pto *in vitro*. **a**, The binding mode of the AvrPto–Pto complex is similar to that of the PKA–PKI complex. Structural alignment of the AvrPto–Pto complex with PKA–PKI complex. Only the GINP loop is shown in AvrPto. **b**, The Pto autophosphorylation activity is inhibited by AvrPto *in vitro*. **c**, Pto phosphorylation of Pti1 is inhibited by AvrPto *in vitro*. Pti1(K96Q) was used as the substrate of Pto. **d**, **e**, Mutations in AvrPto (**d**) and Pto (**e**) that disrupt the AvrPto–Pto interaction impair the kinase inhibition activity of AvrPto. Longer exposure was used for panel **e** than for panel **b**.

Inhibition of the Pto kinase activity by AvrPto is not the signal to initiate a hypersensitive response. However, the kinase inhibition activity of AvrPto can be important for its virulence function. This possibility gains support from a recent study showing that AvrPto and AvrPtoB act as suppressors of an early signalling component(s) upstream of the MAPK cascade that is activated on perception of the bacterial flagellar peptide by the receptor kinase FLS2 in *Arabidopsis*[16]. Suppression of MAPK signalling by AvrPto can be relieved by overexpression of Pto and FLS2. Therefore, Pto-like kinases or Pto-like receptor kinases were suggested to be the virulence targets of AvrPto or AvrPtoB[16]. Functional mimicry of host proteins is an important mechanism used by microbial pathogens to modulate host cellular functions[25]. Accordingly, it is conceivable that some host proteins may have evolved to deceive pathogens by mimicking their virulence targets and then initiating defences when targeted. This explains why the active conformation of Pto is required for interaction with AvrPto (Fig. 2).

METHODS SUMMARY

Protein expression, protein–protein interaction and phosphorylation assays. AvrPto (residues 29–131) in pET30 (Novagen) and the full-length Pto in pGEX-2T (Pharmacia) were co-expressed in *E. coli* strain BL21(DE3). The soluble fraction of the AvrPto–Pto complex was purified using an affinity column and further cleaned by anion-exchange column and gel filtration chromatography. Size exclusion chromatography was employed to detect AvrPto–Pto interaction. Aliquots of peak fraction corresponding to the position of AvrPto–Pto complex were subjected to SDS-polyacrylamide gel electrophoresis. The proteins were visualized by Coomassie blue staining. Buffer containing 20 mM Tris-HCl (pH 7.2), 2 mM dithiothreitol, 5 mM $MgCl_2$ and 10 μM ATP, 2 μCi [γ-^{32}P] (5,000 Ci mmole^{-1}) was used for Pto autophosphorylation and phosphorylation of the substrate Pti1. All the reactions were incubated at 30 °C for 30 min and terminated by adding an equal volume (50 μl) of 2× SDS buffer. SDS-polyacrylamide gel electrophoresis was used to fractionate proteins, and the phosphorylated proteins were visualized using a phosphoimager.

Crystallography. Crystals of the AvrPto–Pto complex were grown using hanging drop vapour diffusion. The native (3.2 Å) and MAD (4.0 Å) data sets for these crystals were collected at the BSRF (Beijing, China) beam line 3W1A using a CCD detector and processed using the software DENZO and Scalepack[26]. The AvrPto–Pto crystal structure was determined by MAD. The ordered selenium sites were positioned and refined by SOLVE/RESOLVE[27]. The experimental electron density was sufficient for model-building with the program O[28] and structure refinement with REFMAC5 (ref. 29). Statistics are given in Supplementary Table 1.

Full Methods and any associated references are available in the online version of the paper at www.nature.com/nature.

Received 5 July; accepted 24 July 2007.
Published online 12 August 2007.

1. Flor, H. H. Current status of the gene-for-gene concept. *Annu. Rev. Phytopathol.* **9**, 275–296 (1971).
2. Belkhadir, Y., Subramaniam, R. & Dangl, J. L. Plant disease resistance protein signaling: NBS-LRR proteins and their partners. *Curr. Opin. Plant Biol.* **7**, 391–399 (2004).
3. Chisholm, S. T., Coaker, G., Day, B. & Staskawicz, B. J. Host–microbe interactions: shaping the evolution of the plant immune response. *Cell* **124**, 803–814 (2006).
4. Innes, R. W. Guarding the goods. New insights into the central alarm system of plants. *Plant Physiol.* **135**, 695–701 (2004).
5. Pedley, K. F. & Martin, G. B. Molecular basis of Pto-mediated resistance to bacterial speck disease in tomato. *Annu. Rev. Phytopathol.* **41**, 215–243 (2003).
6. Scofield, S. R. *et al.* Molecular basis of gene-for-gene specificity in bacterial speck disease of tomato. *Science* **274**, 2063–2065 (1996).
7. Tang, X. *et al.* Initiation of plant disease resistance by physical interaction of AvrPto and Pto kinase. *Science* **274**, 2060–2063 (1996).
8. Salmeron, J. M. *et al.* Tomato Prf is a member of the leucine-rich repeat class of plant disease resistance genes and lies embedded within the Pto kinase gene cluster. *Cell* **86**, 123–133 (1996).
9. He, S. Y., Nomura, K. & Whittam, T. Type III secretion in mammalian and plant pathogens. *Biochim. Biophys. Acta* **1694**, 181–206 (2004).
10. Galan, J. E. *Salmonella* interactions with host cells: type III secretion at work. *Annu. Rev. Cell Dev. Biol.* **17**, 53–86 (2001).
11. Hueck, C. J. Type III protein secretion systems in bacterial pathogens of animals and plants. *Microbiol. Mol. Biol. Rev.* **62**, 379–433 (1998).
12. Kim, Y. J., Lin, N. C. & Martin, G. B. Two distinct *Pseudomonas* effector proteins interact with the Pto kinase and activate plant immunity. *Cell* **109**, 589–598 (2002).
13. Mucyn, T. S. *et al.* The tomato NBARC-LRR protein Prf interacts with Pto kinase *in vivo* to regulate specific plant immunity. *Plant Cell* **18**, 2792–2806 (2006).
14. Rathjen, J. P., Chang, J. H., Staskawicz, B. J. & Michelmore, R. W. Constitutively active Pto induces a Prf-dependent hypersensitive response in the absence of AvrPto. *EMBO J.* **18**, 3232–3240 (1999).
15. Wu, A. J., Andriotis, V. M., Durrant, M. C. & Rathjen, J. P. A patch of surface-exposed residues mediates negative regulation of immune signaling by tomato Pto kinase. *Plant Cell* **16**, 2809–2821 (2004).
16. He, P. *et al.* Specific bacterial suppressors of MAMP signaling upstream of MAPKKK in *Arabidopsis* innate immunity. *Cell* **125**, 563–575 (2006).
17. Wulf, J., Pascuzzi, P. E., Fahmy, A., Martin, G. B. & Nicholson, L. K. The solution structure of type III effector protein AvrPto reveals conformational and dynamic features important for plant pathogenesis. *Structure* **12**, 1257–1268 (2004).

18. Chang, J. H. *et al.* Functional analyses of the Pto resistance gene family in tomato and the identification of a minor resistance determinant in a susceptible haplotype. *Mol. Plant Microbe Interact.* **15,** 281–291 (2002).
19. Frederick, R. D., Thilmony, R. L., Sessa, G. & Martin, G. B. Recognition specificity for the bacterial avirulence protein AvrPto is determined by Thr-204 in the activation loop of the tomato Pto kinase. *Mol. Cell* **2,** 241–245 (1998).
20. Riely, B. K. & Martin, G. B. Ancient origin of pathogen recognition specificity conferred by the tomato disease resistance gene *Pto*. *Proc. Natl Acad. Sci. USA* **98,** 2059–2064 (2001).
21. Huse, M. & Kuriyan, J. The conformational plasticity of protein kinases. *Cell* **109,** 275–282 (2002).
22. Nolen, B., Taylor, S. & Ghosh, G. Regulation of protein kinases; controlling activity through activation segment conformation. *Mol. Cell* **15,** 661–675 (2004).
23. Sessa, G., D'Ascenzo, M. & Martin, G. B. Thr38 and Ser198 are Pto autophosphorylation sites required for the AvrPto–Pto-mediated hypersensitive response. *EMBO J.* **19,** 2257–2269 (2000).
24. Bossemeyer, D., Engh, R. A., Kinzel, V., Ponstingl, H. & Huber, R. Phosphotransferase and substrate binding mechanism of the cAMP-dependent protein kinase catalytic subunit from porcine heart as deduced from the 2.0 Å structure of the complex with Mn^{2+} adenylyl imidodiphosphate and inhibitor peptide PKI(5–24). *EMBO J.* **12,** 849–859 (1993).
25. Stebbins, C. E. & Galan, J. E. Maintenance of an unfolded polypeptide by a cognate chaperone in bacterial type III secretion. *Nature* **414,** 77–81 (2001).
26. Otwinowski, Z. & Minor, W. Processing of X-ray diffraction data collected in oscillation mode. *Methods Enzymol.* **276,** 307–326 (1997).
27. Terwilliger, T. C. SOLVE and RESOLVE: automated structure solution and density modification. *Methods Enzymol.* **374,** 22–37 (2003).
28. Jones, T. A., Zou, J. Y., Cowan, S. W. & Kjeldgaard, M. Improved methods for building protein models in electron density maps and the location of errors in these models. *Acta Crystallogr. A* **47,** 110–119 (1997).
29. Murshudov, G. N., Vagin, A. A. & Dodson, E. J. Refinement of macromolecular structures by the maximum-likelihood method. *Acta Crystallogr.* **D53,** 240–255 (1997).

Supplementary Information is linked to the online version of the paper at www.nature.com/nature.

Acknowledgements We thank R. Innes, S. He and X. Tang for critical reading and comments on our manuscript, and Y. Dong and P. Liu at the BSRF (Beijing, China) beam line 3W1A for assistance with the data collection. We are grateful to X. Liu and L. Ma for help with SPR assay. This research is funded by a Chinese Ministry of Science and Technology grant to J.C. and to J.-M.Z.

Author Contributions W.X. purified, crystallized and determined the structure and performed biochemical assays; Y.Z. performed *Agrobacterium*-mediated transient expression; Q.L., Q. Huang and Q. Hao determined structure; J.L. and X.L. purified proteins; S.C. performed the mass spectrometry assay; J.-W.W. measured the half-maximal inhibitory concentration; R.B. and L.Z. were involved in the study design; and J.-M.Z. and J.C. designed the study, analysed data and prepared the manuscript.

Author Information The atomic coordinates and structure factors of the AvrPto–Pto complex have been deposited in the RCSB Protein Data Bank under accession code 2QKW. Reprints and permissions information is available at www.nature.com/reprints. The authors declare no competing financial interests. Correspondence and requests for materials should be addressed to J.C. (chaijijie@nibs.ac.cn).

METHODS

Protein preparation. Cells expressing AvrPto and Pto were induced with 1 mM IPTG for 10 h at room temperature. Cells were collected, pelleted and then resuspended in buffer A (50 mM Tris, pH 8.0, 100 mM NaCl), supplemented with protease inhibitors. The cells were lysed by sonication and then centrifuged at 14,000 r.p.m. for 1 h. The soluble fraction of the AvrPto–Pto complex from co-expression was purified using Glutathione Sepharose 4B (GS4B) and further cleaned using an anion-exchange column (Source-15Q, Pharmacia) and gel filtration chromatography after removal of GST (Superdex200, Pharmacia). A similar method was used to purify the free forms of AvrPto and Pto, including their various mutants. The unique NCBI identifiers for the proteins are: Pto, A49332; AvrPto, AAA25728; Prf, AAC49408; Pti1, AAC61805; PKA, P36887; PKI, NP_006814; CHK1, AAC51736; TβRI, AAH71181.

Crystallization and data collection. Crystallization conditions for the AvrPto–Pto complex were determined from the sparse matrix screen (Hamptonresearch). Screening was done using hanging drop vapour diffusion by combining 2 μl of protein solution. The buffer containing 0.2 M potassium sodium tartrate, 0.1 M tri-sodium citrate, pH 5.6, and 2.0 M ammonium sulphate generated crystals, which were further optimized by adding 10 mM taurine (2-aminoethanesulfonic acid). Crystals grew to their maximum size ($0.3 \times 0.4 \times 0.5\ mm^3$) approximately within two days. The crystals were transferred to the mother liquor, containing 25% glycerol, then flash cooled in liquid nitrogen. The multiple anomalous dispersion (MAD) data sets from the selenium crystal were collected to 4.0 Å. The crystal belongs to space group $P2_12_12_1$ with cell dimensions $a = 75.465$ Å, $b = 94.591$ Å, $c = 98.741$ Å, and contains one AvrPto–Pto complex per asymmetric unit.

Structure determination and refinement of the AvrPto–Pto complex. All the residues except the first 29 residues of Pto were built for the AvrPto–Pto complex. When justified by the electron density, the phosphate group in the phosphorylated T199 in Pto was included. The final atomic model of AvrPto–Pto was refined to a crystallographic R_{work} of 27.1% and an R_{free} of 30.3% to 3.2 Å. There were no outliers in the Ramachandran plot (79.1%, 16.3%, 4.6% in the core, allowed and generously allowed regions, respectively).

Gel filtration assay for protein–protein interaction. The Pto and AvrPto proteins purified by affinity chromatography and anion-exchange column (Source-15Q, Pharmacia) were used for interaction assay. To examine the interaction between Pto and AvrPto, size exclusion chromatography (Superdex-200 column, Pharmacia Biotech) was employed. In all test runs, AvrPto and Pto were mixed together and incubated at 4 °C for 1 h. Buffer containing 25.0 mM Tris, pH 8.0, 100 mM NaCl, 3 mM dithiothreitol was used for gel filtration assays, with the flow rate of 0.5 ml min^{-1}, unless indicated otherwise. Aliquots of peak fraction corresponding to the position of the AvrPto–Pto complex were subjected to SDS-polyacrylamide gel electrophoresis. The proteins were visualized by Coomassie blue staining.

***In vitro* kinase assay.** For autophosphorylation, 1.5 μg of Pto was diluted to 50 μl using the reaction buffer. For phosphorylation of Pti1(K96Q), 1.5 μg of Pto and 5.0 μg of Pti1(K96Q) were mixed in 50 μl of reaction buffer. To determine the effect of AvrPto on Pto kinase activity, the autophosphorylation and Pti1 phosphorylation assays were carried out in the presence of different concentration of AvrPto (0.8 μg, 1.0 μg, 1.2 μg, 2 μg, 4 μg, 8 μg).

Plasmid constructs and *Agrobacterium*-mediated transient expression. For Pto expression, the *Pto* promoter was PCR-amplified from PtoR tomato plants, digested with *Sac*I and *Eco*RI, and inserted into pFAST (a gift from Y. Xia). The wild-type and mutant *Pto* sequences were PCR amplified, digested with *Bam*HI and *Xho*I, and inserted into the plasmid containing the *Pto* promoter. For AvrPto transient expression, the wild-type and mutant *AvrPto* sequences were PCR-amplified, digested with *Nde*I and *Xho*I, and inserted into the pBTEX plasmid. *Agrobacterium tumefaciens* strain GV3101 containing the binary plasmid of interest was grown in LB media with appropriate antibiotics to stationary phase at 28 degrees. A tenfold dilution was made for the cell cultures with fresh LB plus antibiotics, 10 mM MES, pH 5.6, and 50 μM acetosyringone. These diluted cells were allowed to grow overnight at 28 °C, pelleted and washed once using infiltration medium (MS medium containing 10 mM MES, pH 5.6, and 150 μM acetosyringone). Finally, the cells were resuspended to an OD_{600} of 0.5 using the same medium and injected into *Nicotiana benthamiana* six- to seven-week-old plants. To allow the development of a hypersensitive response, these plants were covered and left in the growth chamber for 4 days.